Sliding-Mode MRA Observer-based Model Predictive Current Control for PMSM Drive system with DC-link voltage Sensorless

Qingfang Teng[1], Jie Tian[1], Junyi Duan[2], Hongwei Cui[1] , Jianguo Zhu[3], and Youguang Guo[3]

[1] Department of Automation and Electrical Engineering, Lanzhou Jiaotong University, Lanzhou Gansu 730070, China
[2] Graduate Management Team Department, Engineering University of Armed Police Force, Xi'an Shaanxi 710000, China
[3] Faculty of Engineering and Information Technology, University of Technology, Sydney, 2007, Australia
Email: tengqf@mail.lzjtu.cn

Abstract--A sliding-mode model reference adaptive (MRA) observer-based model predictive current control (MPCC) strategy is developed for permanent magnet synchronous motor (PMSM) drive systems with DC-link voltage sensorless. Generally a DC-link voltage sensor is indispensable for PMSM drive fed by voltage source inverter (VSI) to implement MPCC. In response to DC-link voltage sensor fault, by combination of MRA and sliding-mode techniques, a novel sliding-mode MRA observer for estimating DC-link voltage is proposed to perform MPCC. Moreover, in view of the variation of system parameters and external disturbance, a new nonlinear exponential function-based sliding-mode (NEFSM) speed regulator is synthesized to enhance the system robustness. In order to reduce the drive current ripple and improve speed & torque control performance, MPCC strategy is employed. The resultant NEFSM-based MPCC PMSM drive system with sliding-mode MRA Observer has excellent dynamical performance. In comparison with PI-based MPCC PMSM drive system with sliding-mode MRA observer, the proposed NEFSM-based one possesses better dynamical response and stronger robustness in the presence of variation of load torque. Numerical simulation validates the feasibility and effectiveness of the proposed scheme.

Index Terms--DC-link voltage sensorless, Model predictive current control, Permanent magnet synchronous motor, Sliding-mode model reference adaptive observer

I. INTRODUCTION

For PMSM drive fed by voltage source inverter (VSI), whether model predictive control (MPC) method or SVPWM modulation is employed, the accurate knowledge of the DC-link voltage of VSI is required to deliver high performance. The output voltage of VSI is in fact dependent to the accuracy of the DC-link voltage sensor. Nevertheless due to sudden failure of the DC-link voltage sensor, the real value of DC-link voltage could not been measured, which would result in motor current cannot follow its desired reference and thus jeopardize overall system operation. It is expected that drive system maintains satisfactory operation even in the event of DC-link voltage sensor fault. Therefore, DC-link voltage sensor fault tolerant is highly desirable. On the other hand, in some applications, it is generally assumed that the DC-link voltage is known or constant, i.e. DC-link voltage is used by its nominal value. This is not right and is unacceptable for many applications like hybrid electric vehicles (HEVs) and wind turbine three-phase or PV single-phase grid-connected converters whereby the DC-link voltage fluctuates considerably. As described in the end, it is essential to research fault-tolerant operation of DC-link voltage sensor or real-time DC-link voltage observer.

As for the aforementioned fault-tolerant method, there are two solutions, one being hardware-based redundancy and the other being software-based algorithm which is known as sensorless method. It is known that high DC-link voltage sensor's cost itself is high, and adding such redundant sensor to system necessarily increases higher cost and greater hardware complexity and bigger size. So the first solution is impracticable. While digital signal processors have become more attractive because of their comparative low-cost and easy implementation of complex control strategies, hence the second solution has been highly praising.

Over the past years, a few DC-link voltage sensorless methods have been reported in the field of grid-connected inverters and HEVs electrical drives as well as VSI-based drives [1]-[5]. For a three-phase grid-connected inverter, the predictive current-based DC-link voltage is obtained from inverter · output current information [1]. This approach involves with three AC voltage sensors and two AC current sensors used for measuring grid voltages and inverter output currents, respectively, therefore its system structure is complex. For battery charger used in automotive systems, by model reference adaptive (MRA) technique, [2] proposes the estimations of DC-link voltage in traction and charger modes, respectively. Because the designed observer deals with the information of real-time PWM duty cycles which, however, is obtained by using experimental data collected on an off-line test bed, its implementation is difficult. For single-phase grid-connected photovoltaic converters, by guaranteeing that the tracked PV maximum power is transferred to the grid, power balance is achieved at the inverter DC-link, and thus DC-link voltage is stabilized by nature without the need of DC-link voltage controller [3]. However, it is not suitable for motor drive systems. For induction motor and PMSM drive systems, MRA method is employed to design an online DC-link voltage observer [4]-[5], but there is a noticeable problem in their design processes. Their common issue lies in that the

outputs of controller are regarded as the inputs of observer. Concretely speaking, for [4], the input voltage provided for observer comes from the output of controller. However, from its reasoning process of observe, it is proved that the input voltage supplied to observer should be the motor stator one when the DC-link voltage is its nominal value. For [5], the direct and quadratic-axis voltages supplied to observer are stator voltage references coming from the output of PI current controllers. Nevertheless, from its theoretical derivation process of observer, it is shown that the two voltages supplied to observer should be motor direct and quadratic-axis ones when the DC-link voltage is its nominal value. On the other hand, although MRA-based observer is relatively easy to implement, its estimation accuracy heavily depends on the motor parameters to some extent. When motor parameter variations or external disturbance occurs, it may not be applicable.

It is well known that sliding-mode (SM) control has strong anti-interference capability, therefore SM technique can be incorporated into MRA-based observer. Nevertheless conventional SM may bring unsatisfactory chattering due to switch function. To weaken chattering, nonlinear exponential function can be used instead of switch function. With making use of advantages of MRA and nonlinear exponential function-based SM, a novel SM-based MRA observer is investigated in this paper. The proposed observer can increase DC-link voltage estimation accuracy and robustness. So far there is no literature on such observer.

For PMSM drive systems, model predictive current control (MPCC) is an emerging control strategy and has been arousing significant attention from electrical drives community, which adopts the principles of MPC. It achieves the stator current to track its reference value accurately with short transient interval, and thus plays an important role in high-performance PMSM drives to ensure the quality of the torque and speed control.

For conventional MPCC PMSM drive system, its speed regulator employs PI algorithm which doesn't work properly whenever the variation of system parameters and external disturbances occur. To improve its robustness, a new nonlinear exponential function-based sliding-mode (NEFSM) speed regulator is put forward in this paper. The NEFSM regulator can enable drive system not only to be superior robust against system uncertainties and external disturbances but also to have quick response as well as high control precision. Now, studies on NEFSM regulator are little. In this paper, we replace PI with NEFSM for MPCC PMSM drive system.

In this paper, a novel sliding-mode MRAS observer with quick and accurate estimation of DC-link voltage is introduced. Its adaptation law is determined to guarantee its stability. The designed observer is fed by motor speed and stator currents as well as the direct and quadratic axes stator voltages on condition that DC-link voltage is its nominal value. Estimated DC-link voltage is applied to MPCC. The proposed observer can be utilized in DC-link

voltage sensorless or fault resilient PMSM drive system. Meanwhile a new NEFSM controller is designed to enhance the speed regulator's robustness against parameter uncertainty and external disturbance and its stability is proved as well. With combination of the sliding-mode MRA observer and NEFSM methods aforementioned, the synthesized NEFSM-based MPCC PMSM drive system with DC-link voltage sensorless achieves satisfactory dynamical and steady-state performance.

This paper is organized as follows: dynamic model of PMSM drive is presented in Section II. Section III gives the sliding-mode MRA observer and NEFSM speed regulator design as well as MPCC design. Experimental results and analysis are presented in Section IV. Section V contains the conclusion.

II. Dynamic Model of PMSM Drives

As for three-phase surface-mounted PMSM drive, $L_d = L_q = L$, the model in rotor synchronous reference frame (dq-frame) is expressed as follows

$$\begin{cases} \dfrac{di_d}{dt} = \dfrac{1}{L_d}(u_d - R_s i_d + p\omega_r L_q i_q) \\ \dfrac{di_q}{dt} = \dfrac{1}{L_q}(u_q - R_s i_q - p\omega_r(L_d i_d + \psi_f)) \end{cases} \tag{1}$$

where R_s is stator resistance, L_d, L_q are d-axis and q-axis stator inductances, Ψ_r is permanent magnet flux, u_d, u_q are d-axis and q-axis stator voltages, i_d, i_q are d-axis and q-axis stator currents, ω_r is mechanical rotor speed, p is number of pole pairs.

The mechanical equation is expressed as

$$J\frac{d\omega_r}{dt} = T_e - T_l - B_m\omega_r - T_f \tag{2}$$

Where J is inertia of moment, T_e, T_l are electromagnetic and load torque, T_f is coulomb friction torque, B_m is viscous friction coefficient.

And the electromagnetic torque T_e is expressed as

$$T_e = \frac{3p}{2}\left[\psi_f i_q + \left(L_d - L_q\right)i_d i_q\right] \tag{3}$$

III. Design of NEFSM-based MPCC PMSM Drive System with DC-link Voltage Sensorless

The objective of NEFSM-based MPCC with DC-link voltage sensorless is that the PMSM drive system can work reliably and its speed and torque can be controlled not only to have satisfactory performance but also to be strong robust to parameters variation and external disturbance. The schematic of the proposed control system is shown in Fig.1.Our design task concentrates on DC-link voltage observer, NEFSM speed regulator and MPCC.

A. Sliding-mode MRA observer design

The proposed observer is to estimate DC-link voltage. For PMSM driven by a 2-level 3-phase VSI [6]-[7], six nonzero stator voltage space vectors can be generated by
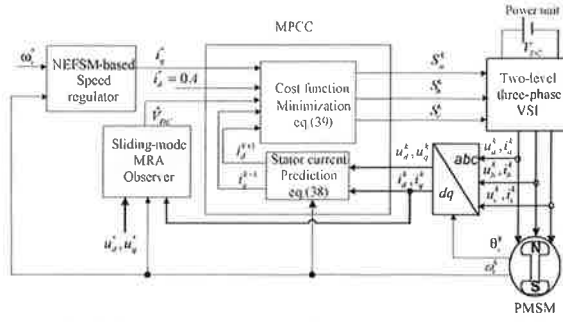
Fig.1. Block diagram of NEFSM-based MPCC PMSM drive system with DC-link voltage sensorless

controlling its switches states. The actual magnitude of every stator voltage vector is given by

$$u_s = 2V_{DC}/3 \qquad (4)$$

where V_{DC} is the actual DC-link voltage. If DC-link voltage is nominal value, the corresponding stator voltage is calculated by

$$u_s^* = 2V_{DC(nom)}/3 \qquad (5)$$

where $V_{DC(nom)}$ is the nominal value of DC-link voltage. Define the coefficient

$$\alpha = V_{DC}/V_{DC(nom)} \qquad (6)$$

Accordingly, the actual stator voltage can be gotten by

$$u_s = \alpha u_s^* \qquad (7)$$

And then there exists following expression

$$u_d = \alpha u_d^*, \quad u_q = \alpha u_q^* \qquad (8)$$

where u_d^* and u_q^* are the d-axis and q-axis voltages corresponding to u_s^* when DC-link voltage is $V_{DC(nom)}$.

When DC-link voltage sensor is out of order, actual DC-link voltage is not measurable. By means of designing sliding-mode MRA observer, the estimated value of α can be obtained, and then the estimated value of the actual DC-link voltage can be determined as below

$$\hat{V}_{DC} = \hat{\alpha} V_{DC(nom)} \qquad (9)$$

where $\hat{\bullet}$ denotes estimated value of $\bullet$.

(1) MRA Observer

1) MRA observer design

The estimated value of α is obtained by MRA observer, which consists of a reference model and an adjustable model. From (1), the reference model is represented by

$$\begin{bmatrix} \dfrac{di_d'}{dt} \\ \dfrac{di_q'}{dt} \end{bmatrix} = \begin{bmatrix} -\dfrac{R_s}{L} & p\omega_r \\ -p\omega_r & -\dfrac{R_s}{L} \end{bmatrix} \begin{bmatrix} i_d' \\ i_q' \end{bmatrix} + \dfrac{1}{L}\begin{bmatrix} u_d' \\ u_q' \end{bmatrix} \qquad (10)$$

where

$$\begin{bmatrix} u_d' \\ u_q' \end{bmatrix} = \begin{bmatrix} u_d + R_s\psi_f/L \\ u_q \end{bmatrix} = \begin{bmatrix} \alpha u_d^* + R_s\psi_f/L \\ \alpha u_q^* \end{bmatrix}$$

$$\begin{bmatrix} i_d' \\ i_q' \end{bmatrix} = \begin{bmatrix} i_d + \psi_f/L \\ i_q \end{bmatrix}$$

Then the adjustable model can be constructed as

$$\begin{bmatrix} \dfrac{d\hat{i}_d'}{dt} \\ \dfrac{d\hat{i}_q'}{dt} \end{bmatrix} = \begin{bmatrix} -\dfrac{R_s}{L} & p\omega_r \\ -p\omega_r & -\dfrac{R_s}{L} \end{bmatrix} \begin{bmatrix} \hat{i}_d' \\ \hat{i}_q' \end{bmatrix} + \dfrac{1}{L}\begin{bmatrix} \hat{u}_d' \\ \hat{u}_q' \end{bmatrix} + k_1\begin{bmatrix} i_d' - \hat{i}_d' \\ i_q' - \hat{i}_q' \end{bmatrix} \qquad (11)$$

where $\hat{\bullet}$ denotes estimate of $\bullet$ and k_1 is observer gain.

$$\begin{bmatrix} \hat{u}_d' \\ \hat{u}_q' \end{bmatrix} = \begin{bmatrix} \hat{u}_d + R_s\psi_f/L \\ \hat{u}_q \end{bmatrix} = \begin{bmatrix} \hat{\alpha} u_d^* + R_s\psi_f/L \\ \hat{\alpha} u_q^* \end{bmatrix}$$

Subtracting (11) from (10), we have following error equation

$$\begin{bmatrix} \dfrac{d\tilde{i}_d'}{dt} \\ \dfrac{d\tilde{i}_q'}{dt} \end{bmatrix} = \begin{bmatrix} -\dfrac{R_s}{L} & p\omega_r \\ -p\omega_r & -\dfrac{R_s}{L} \end{bmatrix} \begin{bmatrix} \tilde{i}_d' \\ \tilde{i}_q' \end{bmatrix} + \dfrac{\tilde{\alpha}}{L}\begin{bmatrix} u_d^* \\ u_q^* \end{bmatrix} - k_1\begin{bmatrix} \tilde{i}_d' \\ \tilde{i}_q' \end{bmatrix}$$

$$= \begin{bmatrix} -\dfrac{R_s}{L} - k_1 & p\omega_r \\ -p\omega_r & -\dfrac{R_s}{L} - k_1 \end{bmatrix} \begin{bmatrix} \tilde{i}_d' \\ \tilde{i}_q' \end{bmatrix} + \dfrac{\tilde{\alpha}}{L}\begin{bmatrix} u_d^* \\ u_q^* \end{bmatrix} \qquad (12)$$

Where $\tilde{\bullet}$ denotes $(\bullet - \hat{\bullet})$.

2) Stability analysis and MRA law

In order to guarantee the stability of (12) and obtain adaptive mechanism, let us define the candidate Lyapunov function (CLF) as below

$$V_1 = \left(\tilde{i}_d'^2 + \tilde{i}_q'^2 + k_2\tilde{\alpha}^2\right)/2 \geq 0 \qquad (13)$$

Where k_2 is a positive constant.
The derivative of (13) is

$$\dot{V}_1 = -\left(R_s/L + k_1\right)\tilde{i}_d'^2 - \left(R_s/L + k_1\right)\tilde{i}_q'^2 + \dfrac{1}{L}u_d^*\tilde{i}_d'\tilde{\alpha} + \dfrac{1}{L}u_q^*\tilde{i}_q'\tilde{\alpha} + k_2\tilde{\alpha}\dfrac{d\tilde{\alpha}}{dt} \qquad (14)$$

To make error dynamic system (12) to be stable, dV_1/dt should be less than zero. Hence assume following inequation

$$\dfrac{1}{L}u_d^*\tilde{i}_d'\tilde{\alpha} + \dfrac{1}{L}u_q^*\tilde{i}_q'\tilde{\alpha} + k_2\tilde{\alpha}\dfrac{d\tilde{\alpha}}{dt} = 0 \qquad (15)$$

Thus (15) can be rewritten as

$$\dfrac{d\tilde{\alpha}}{dt} = -\dfrac{1}{k_2 L}\left(u_d^*\tilde{i}_d' + u_q^*\tilde{i}_q'\right)$$

Because the variation rate of DC-link voltage is very slow, $d\alpha/dt \approx 0$ is workable and thus MRA law is obtained as following

$$\hat{\alpha} = \int\left(u_d^*\tilde{i}_d' + u_q^*\tilde{i}_q'\right)dt/k_2 L \qquad (16)$$

For improving the estimation accuracy of α and ensuring its null steady error, the PI-based MRA law is employed

$$\hat{\alpha} = k_p\left(u_d^*\tilde{i}_d' + u_q^*\tilde{i}_q'\right) + k_i\int\left(u_d^*\tilde{i}_d' + u_q^*\tilde{i}_q'\right)dt \qquad (17)$$

Where k_p and k_i are proportional and integral constants.

(2) Sliding- mode MRA Observer

1) Sliding- mode MRA observer design

To increase the observer robustness against system disturbance, sliding-mode variable structure technique is incorporated into the MRA-based observer.

The sliding surface is selected as

$$S = k_p \left(u_d^* \tilde{i}_d^{\prime\prime} + u_q^* \tilde{i}_q^{\prime\prime} \right) + k_i \int \left(u_d^* \tilde{i}_d^{\prime\prime} + u_q^* \tilde{i}_q^{\prime\prime} \right) dt$$
$$= k_p (e_{dq} + k_{ip} \int e_{dq} \, dt) \tag{18}$$

where $k_{ip} = k_i / k_p$ and e_{dq} is expressed as

$$e_{dq} = u_d^* \tilde{i}_d^{\prime\prime} + u_q^* \tilde{i}_q^{\prime\prime} \tag{19}$$

Then the sliding-mode MRA observer is designed as

$$\hat{\alpha} = k_s \, \text{sgn}(S) \tag{20}$$

where k_s is sliding-mode gain, sgn( ) is switch function.
In fact, (20) is a conventional sliding-mode observer, in which the sign function may incur chattering. To weaken chattering, the sign function in (20) can be replaced by a nonlinear exponential function as follows

$$\text{fal}(x, \varepsilon, \delta) = \begin{cases} \dfrac{x}{\delta^{1-\varepsilon}}, |x| \leq \delta; \\ \text{sgn}(x) \cdot |x|^{\varepsilon}, |x| > \delta \end{cases} \tag{21}$$

where δ is filtering factor and ε is nonlinear factor.

From (21), it can be seen that when $\varepsilon < 1$, if error x is small, the gain of (21) will be big, and vice versa. It is the above-mentioned property that can improve the ability to depress disturbance and mitigate chattering [8]. Therefore, by substituting for (20), the nonlinear exponential function-based sliding-mode MRA observer is expressed as follows

$$\hat{\alpha} = k_s \text{fal}(S, \varepsilon, \delta) \tag{22}$$

Sequentially the actual DC-link voltage can be estimated as

$$\hat{V}_{DC} = \hat{\alpha} V_{DC(nom)} \tag{23}$$

According to the above-mentioned analysis, the block diagram of the sliding-mode MRA observer is shown as in Fig. 2.
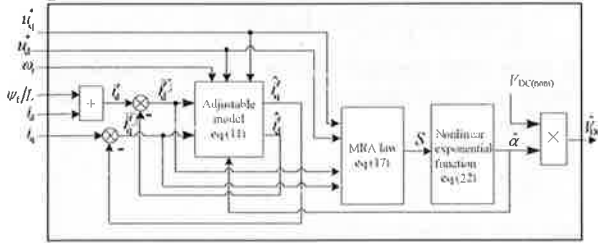

Fig.2. Block diagram of sliding-mode MRA observer

2) Stability analysis
In order to guarantee stability of (22), CLF is selected as

$$V_2 = S^2/2 \tag{24}$$

The derivative of (19) is

$$\dot{e}_{dq} = -\frac{\hat{\alpha}}{L}(u_d^{*2} + u_q^{*2}) + \frac{\alpha}{L}(u_d^{*2} + u_q^{*2}) +$$
$$\tilde{i}_d^{\prime}(\frac{du_d^*}{dt} - \frac{R_s}{L}u_d^* - k_v u_d^* - p\omega_r u_q^*) + \tag{25}$$
$$\tilde{i}_q^{\prime}(\frac{du_q^*}{dt} - \frac{R_s}{L}u_q^* - k_v u_q^* + p\omega_r u_d^*)$$

Let

$$f_1 = \frac{1}{L}(u_d^{*2} + u_q^{*2}) \tag{26}$$

$$f_2 = \frac{\alpha}{L}(u_d^{*2} + u_q^{*2}) + \tilde{i}_d^{\prime}(\frac{du_d^*}{dt} - \frac{R_s}{L}u_d^* - k_v u_d^* - p\omega_r u_q^*) +$$
$$\tilde{i}_q^{\prime}(\frac{du_q^*}{dt} - \frac{R_s}{L}u_q^* - k_v u_q^* + p\omega_r u_d^*) \tag{27}$$

Thus (25) can be rewritten as

$$\dot{e}_{dq} = -\hat{\alpha} f_1 + f_2 \tag{28}$$

Hence the derivative of (24) is

$$\dot{V}_2 = S\dot{S} = k_p S(\dot{e}_{dq} + k_{ip} e_{dq})$$
$$= k_p S(-\hat{\alpha} f_1 + f_2 + k_{ip} e_{dq})$$
$$= k_p S(-k_s \text{fal}(S, \varepsilon, \delta) f_1 + f_2 + k_{ip} e_{dq})$$
$$= k_p [-k_s |S \text{fal}(S, \varepsilon, \delta)| f_1 + S(f_2 + k_{ip} e_{dq})]$$

To make (22) to be stable, dV_2/dt should be less zero. i.e.,

$$k_s |S \text{fal}(S, \varepsilon, \delta)| f_1 > S(f_2 + K_{iq} e_{dq}) \tag{29}$$

Therefore, selecting large enough k_s to satisfy (29) can ensure both the existence of sliding motion and asymptotical stability of sliding motion in the global scope. Once the (22) reaches the sliding surface $S = 0$, then we have

$$\dot{S} = k_p(\dot{e}_{dq} + k_{ip} e_{dq}) = 0 \tag{30}$$

(30) means that e_{dq} can exponentially approach zero. Consequently $\hat{\alpha}$ can rapidly track α and thus the estimated DC-link voltage can track its actual one.

B. NEFSM speed regulator
(1) NEFSM speed regulator design
To enable the drive system to be not only strong robust but also high accuracy, integral sliding mode-based speed regulator is employed.
Define speed error as

$$e_\omega = \omega_r^* - \omega_r \tag{31}$$

where ω_r^* is reference rotor speed.
Integral sliding mode surface is designed as bellow

$$S_\omega = e_\omega + k_3 \int e_\omega \, d\tau \tag{32}$$

where k_3 is a positive integral constant.
Taking the derivative of (32) yields

$$\frac{dS_\omega}{dt} = \dot{\omega}_r^* + k_3 e_\omega - \frac{3p\psi_f}{2J}i_q + \frac{B_m}{J}\omega_r + \frac{T_1 + T_f}{J} \tag{33}$$

To reduce the chattering of conventional sliding mode, a nonlinear exponential reaching law is adopted as

$$\frac{dS_\omega}{dt} = -k_\omega \text{fal}(S_\omega, \varepsilon_1, \delta_1) \tag{34}$$

Where k_w is a positive constant.
Let (33) be equal to (34) and thus the NEFSM law of speed regulator can be obtained

$$i_q^* = \frac{2J}{3p\psi_f}\left[\dot{\omega}_r^* + k_3 e_\omega + \frac{B_m}{J}\omega_r + \frac{T_1 + T_f}{J} + k_\omega \text{fal}(S_\omega, \varepsilon_1, \delta_1)\right] \tag{35}$$

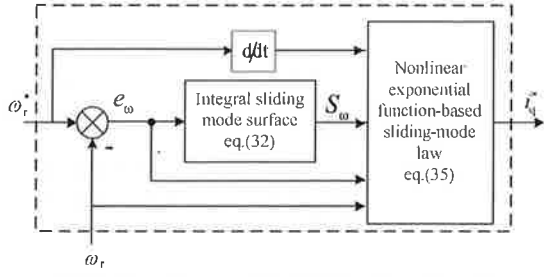By combing (32) and (35), the block diagram of designed NEFSM-based speed regulator is shown as in Fig.3.

Fig.3. Block diagram of NEFSM-based speed regulator

(2) Stability analysis

Define a CLF

$$V_3 = S_\omega^2 / 2 \tag{36}$$

The derivative of (36) is

$$\dot{V}_3 = S_\omega \dot{S}_\omega = -k_\omega \left| S_\omega \mathrm{fal}(S_\omega, \varepsilon_1, \delta_1) \right| \leq 0 \tag{37}$$

By Lyapunov stability theory, NEFSM-based speed regulator (35) is stable.

C. Model predictive current control

The algorithm of MPCC is that by means of the dynamical model of PMSM driven by a 2-level 3-phase VSI, firstly predict the future behavior of *d*-axis and *q*-axis currents for each switching state (i.e. every nonzero stator voltage vector). Secondly evaluate the effect of each stator voltage vector, and finally, select one stator voltage vector such that its corresponding *d*-axis and *q*-axis currents at the end of the cycle are as close as possible to their reference values. MPCC consists of stator currents prediction and cost function minimization.

(1)Predictive model for stator currents

Discretization of (1) yields the prediction of the stator currents at $(k+1)th$ instant as following

$$\begin{cases} i_d^{k+1} = i_d^k + (u_d^k - R_s i_d^k + pL\omega_r^k i_q^k)T_s / L \\ i_q^{k+1} = i_q^k + (u_q^k - R_s i_q^k - p\omega_r^k (Li_d^k + \psi_m))T_s / L \end{cases} \tag{38}$$

(2) Cost function minimization

The minimum value of cost function is defined as

$$\min.\{g_i\} = \left| i_d^* - i_d^{k+1} \right| + k_4 \left| i_q^* - i_q^{k+1} \right| \tag{39}$$

$$s.t.\, u_s^k \in \{V_1 \quad V_2 \quad V_3 \quad V_4 \quad V_5 \quad V_6\}$$

where i_d^* and i_q^* are *d*-axis and *q*-axis stator current reference values, respectively. i_d^{k+1} and i_q^{k+1} are their predictions at $(k+1)th$ instant. k_4 is positive weight value. V_1, V_2, V_3, V_4, V_5 and V_6 are six nonzero voltage vectors generated by 2-level 3-phase VSI. u_s^k is actual stator voltage at *kth* instant which is expressed as

$$u_s^k = 2\hat{V}_{DC}\left[S_a^k + e^{j2\pi/3} S_b^k + e^{-j2\pi/3} S_c^k \right]/3$$

Where $S_x^k(x=a,b,c)$ is upper power switch state of one of three legs at *kth* instant. $S_x^k=1$ or $S_x^k=0$ when upper power switch is on or off. $\hat{V}_{DC}$ is the estimation provided by (23).

In every cycle, by substituting (38) into (39), the optimal stator voltage vector can be found, which will be applied to VSI at $(k+1)th$ instant.

IV. SIMULATION AND ANALYSIS

In order to validate the effective of proposed control scheme, the designed control system as shown in Fig.1

Symbol	Value	Symbol	Value
R_s	2.875Ω	T_n	4N.m
L_d, L_q	0.0085H	n_N	2000rpm
ψ_f	0.175 Wb	J	0.0008Kg.m²
p	4	B_m	0.001N.m.s
$V_{DC(nom)}$	300V	T_J	0

has been implemented in Matlab/Simulink/Simscape platform. The parameters of PMSM are given in Table 1. The sampling period is 26 us, the reference speed n^* is set to 1000rpm. The load torque is increased from 0 N.m to 2 N.m at 0.2 seconds. Let the actual value of DC-link voltage be changed from the given initial value 295V to 315 V at 0.3 seconds. The parameters of sliding-mode MRA observer are tuned as

$$k_1 = 8000, k_p = 0.01, k_i = 0.05, \varepsilon = 0.5, \delta = 0.1, k_s = 3.2$$

The parameters of NEFSM-based speed regulator and MPCC in (39) are tuned as follows,

$$k_3 = 0.001, k_\omega = 900, \varepsilon_1 = 0.5, \delta_1 = 0.1, k_4 = 120$$

A. The NEFSM-based MPCC PMSM drive system comparison between the one with DC-link voltage sensor and the other with DC-link voltage observer

In order to verify estimation accuracy of the designed observer for NEFSM-based MPCC PMSM drive system, two scenarios of numerical simulation are provided, which correspond to PMSM system with DC-link voltage sensor and PMSM system with DC-link voltage observer, respectively. For convenience sake, the former is marked as Case one and the latter one as Case two. Two systems employ completely identical the NEFSM-based MPCC strategy.

Fig.4 shows comparison of two scenarios in terms of DC-link voltage, rotor speed and torque. From Fig.4(a), it can be seen that, for designed observer of Case two, the estimated DC-link voltage rises from its initial value, which is set as 70% of its nominal value, and tracks sensor value of Case one rapidly and accurately. Fig.4(b)-4(c) show that, for Case two, its speed and torque can adapt to whatever the DC-link voltage changes and are almost the same as Case one.
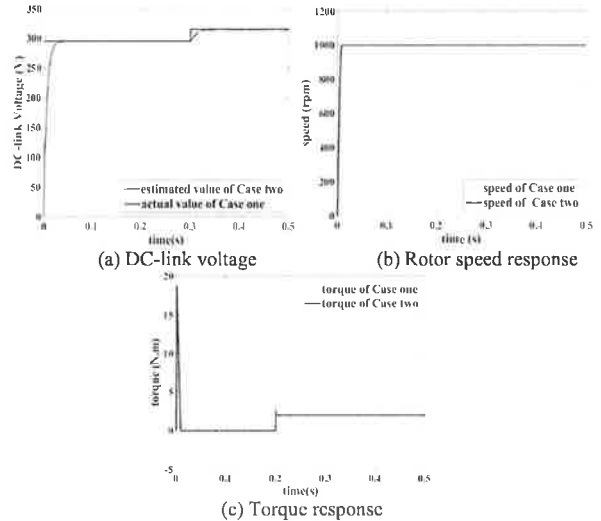

(a) DC-link voltage

(b) Rotor speed response

(c) Torque response

Fig. 4. Dynamic response comparison between Case one and Case two

B. The MPCC PMSM drive system comparison between the one based on PI and the other based on NEFSM speed regulators

(1) The comparison of anti-load variation ability under the same speed transient response

The parameters of PI for PI-based MPCC PMSM system are tuned as follows,

$$K_P = 0.1, K_i = 0.2$$

such that PI-based MPCC system has almost the same speed transient response as NEFSM-based one.

Fig.5 shows their dynamical speed and torque response. Fig.5(a) intuitively gives their speed response comparison, which demonstrates that for NEFSM-based MPCC PMSM system, its speed can sharply adapt to the change of external load in a satisfactory manner, and its capable of accommodating the challenge of load disturbance is superior to PI-based one's. From Fig.5(b), it can be seen that for two systems with the same DC-link observer, their torque responses are almost the same.
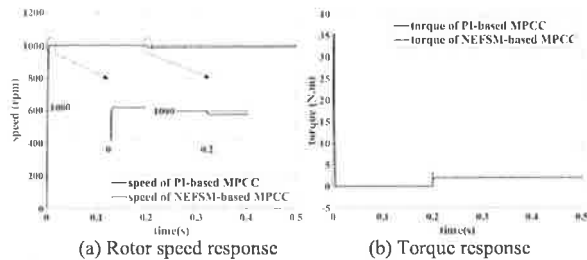

(a) Rotor speed response   (b) Torque response

Fig. 5. Comparison of anti-load variation ability under the same speed transient response

(2) The comparison of dynamic responses under the same anti-load variation ability

The parameters of PI for PI-based MPCC PMSM system are tuned as,

$$K_P = 0.8, K_i = 0.4$$

such that PI-based MPCC system has almost the same anti-load variation ability as NEFSM-based one.

Fig.6 shows their dynamical speed and torque response. Fig. 6(a) intuitively gives their speed response comparison, which indicates that the speed of NEFSM-based MPCC PMSM system has smaller overshoot and faster settling time than one of PI-based system. Meanwhile, it can be found from Fig.6(b) that the torque response of NEFSM-based MPCC PMSM system is better than one of PI-based one.
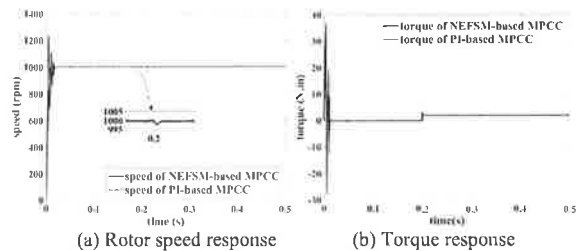

(a) Rotor speed response   (b) Torque response

Fig. 6. The comparison of dynamical response under the same anti-load variation Ability

Summarizing above simulation experiments, we can obtain following results,

- The proposed observer can estimate the actual DC-link voltage rapidly and accurately.
- Compared with PI-based MPCC PMSM drive systems, NEFSM-based one has better dynamical response behavior and stronger robustness.

V. CONCLUSIONS

This paper has put forward a novel NEFSM-based MPCC strategy for PMSM drive system with DC-link voltage observer. The designed SM-based MRA observer is capable of online estimation of the actual DC-link voltage rapidly and accurately and thus can be embedded into a fault resilient PMSM drive system. The designed NEFSM controller can enhance speed regulator's robustness against variation of system parameters and external disturbance. The employed MPCC can reduce the drive current ripple and improve speed & torque control performance. The resultant NEFSM-based MPCC PMSM drive system with sliding-mode MRA Observer achieves not only fast response but also high-precision control performance as well as strong robustness.

REFERENCES

[1] Z. Wang. L. Chang, M. Mao, "Dc voltage sensorless control method for three-phase grid-connected inverters," *IET Power Electron.*, vol.3, no. 4, pp. 552-558, 2010.

[2] S.Diao, D.Diallo, E.Laboure, "A nonlinear observer for DC bus voltage estimation and sensor diagnosis for a battery charger used in automotive systems, " *IEEE 24th International Symposium on Industrial Electronics (ISIE 2015)*, Sep. 2015, pp. 438-443.

[3] N. E. Zakzouk, A. K. Abdelsalam, A. A. Helal, and A.A.Helal, " PV Single-Phase Grid-Connected Converter: DC-Link Voltage Sensorless Prospective," *IEEE Journal of Emerging and Selected Topics in Power Electronics*, vol.5, no.1, pp.526- 546, 2017.

[4] F. R. Salmasi, T. A. Najafabadi, and P. J. Maralani, "An adaptive flux observer with online estimation of DC-link voltage and rotor resistance for VSI-based induction motors," *IEEE Trans. Power Electron.*, vol. 25, no. 5, pp.1310-1319, 2010.

[5] G. F. H. Beng, X.N. Zhang, and D. M. Vilathgamuwa, "Sensor Fault-Resilient Control of Interior Permanent-Magnet Synchronous Motor Drives," *IEEE/ASME Transactions on mechatronics*, vol. 20, no. 2, pp. 855-864, 2015.

[6] Q.F.Teng, J.Y.Bai, J.G.Zhu, et al. "Sensorless model predictive torque control using sliding mode model reference adaptive system observer for permanent magnet synchronous motor drive systems," *Control Theory & Application*, vol. 32, no. 2, pp. 150-161, 2015.

[7] G. Lei, W. Xu, J. F. Hu, J. G. Zhu, Y. G. Guo and K. R. Shao, "Multilevel design optimization of a FSPMM drive system by using sequential subspace optimization method," *IEEE Transactions on Magnetics*, vol. 50, no. 2, 2014, Art. no. 7016904.

[8] J.Q.Han. Active Disturbance Rejection Control Technique—the Technique for Estimating and Compensating the Uncertainties, Beijing: National Defense Industry Press, 2008.